Journal Name

Dynamic Article Links ▶

ARTICLE TYPE

Strategies for optimizing the performance of carbazole thiophene appended unsymmetrical squaraine dyes for dye-sensitized solar cells

Suraj Soman,*,[a] M. A. Rahim,[a] S. Lingamoorthy,[a] Cherumuttathu H. Suresh,[c] and Suresh Das*,[a,b]

Unsymmetrical squaraine dyes (CTSQ-1 and CTSQ-2) with carbazole thiophene donor units were synthesized, characterized and used as sensitizers in dye-sensitized solar cells (DSSCs). These squaraines exhibited intense absorption in the near IR-visible region of the solar spectrum both in solution and on TiO$_2$ surface. The LUMO level of parent sensitizer (CTSQ-2) was positioned at potential much close to the conduction band of TiO$_2$ resulting in lack of enough driving force for electron injection which was modulated by structurally changing the donor carbazole moiety (CTSQ-1), pushing the LUMO more positive thereby enhancing the driving force. Theoretical calculations were carried out in order to have a better understanding of the electron density distribution in CTSQ-1 and CTSQ-2. Electron injection dynamics in CTSQ-1 was studied in detail by changing the Li$^+$ concentration and its effect on photovoltaic parameters were discussed with the help of JV, IPCE, lifetime and EIS measurements.

1. Introduction

Renewable energy technologies will need to play a bigger role in the future than they do today in order to circumvent climate change and fossil fuel depletion.[1,2] One answer to global warming is to replace and retrofit current technologies with alternatives that have comparable or better performance, but do not emit carbon dioxide.[3] Solar energy technologies are poised for significant growth in the 21st century. Photovoltaic solar electricity can deliver and is delivering clean, reliable, on-demand power in current markets worldwide.[4,5] There is a large future market demand for solar photovoltaics; the projection for 2050 varies nearly two orders of magnitude from ca. 100 GW annum^{-1}

[a] Photosciences and Photonics Section, Chemical Science and Technology Division, CSIR-National Institute for Interdisciplinary Science and Technology, Trivandrum, 695 019 and Network of Institutes for Solar Energy (NISE), India. Tel: +91-813918534, E-mail: suraj@niist.res.in

[b] Kerala State Council for Science Technology and Environment, Sasthra Bhavan, Pattom, Thiruvananthapuram 695004, Kerala, India. Tel: +91-9447706202, Fax: +91-471-2540085. E-mail: sureshdas55@gmail.com

[c] Inorganic and Theoretical Chemistry Section, CSIR-National Institute for Interdisciplinary Science and Technology, Trivandrum, 695019, India.

*Corresponding Author

to nearly 10 TW annum^{-1}. Dye-sensitized solar cells (DSSCs) are attracting much attention in comparison with the conventional Si photovoltaics due to its ease of fabrication, low cost, higher efficiencies and short energy payback time.[6,7,8]

In DSSC, sensitizers play a vital role which lead to extensive research in developing new dye molecules to harvest the entire visible and NIR region of sunlight, of these ruthenium polypyridyl complexes, proved to be the most successful ones giving consistent efficiencies above 10%.[4,9] In spite of all these advantages the relatively higher cost and scarcity of Ru metal along with the exhibited absorption limited to the visible range necessitates the need for sensitizers that can absorb in the NIR region. A way to increase the power conversion efficiency is by employing dyes that have panchromatic absorption along with high molar extension coefficients.

Metal free organic dyes proved to be alternative sources for the metal bound sensitizers owing to their higher molar absorption coefficients, tunable photophysical and electrochemical properties, ease of structural modifications and cost effectiveness.[10] Grätzel *et al.* recently reported 13% efficiency for a Zn porphyrin dye (SM 315) with an alternate Co (II/III) redox shuttle. Among the metal free dyes squaraines are well known for intense absorption in the NIR region and flexibility for synthetic modifications.[11] Most of these dyes were synthesized by the condensation of squaric acid with various kinds of aromatic and heterocyclic compounds. A range of squaraine dyes both

symmetrical and unsymmetrical have been reported as efficient sensitizers for DSSC.[12] Alex *et al.* in 2005 initiated the studies on unsymmetrical squaraine dyes and showed that the unidirectional electron flow from donor to acceptor is more promoted in unsymmetrical squaraines than symmetrical squaraines where the excited state electron density used to get localized more on the cyclobutene ring.[13] Recently Grätzel's group reported 7.3% efficiency for a particular class of unsymmetrical squaraines.[14,15]

In the present paper, we report the synthesis, characterization and photovoltaic performance of two unsymmetrical squaraine sensitizers. These dyes are characterized by a carbazole thiophene donor unit and an indolium acceptor unit. Further, a carboxylic acid moiety is used as an anchoring group to bind these dyes to TiO_2 surface. Carbazole moieties are proved to be efficient electron donor groups for enhancing the light harvesting capability of sensitizers in metal containing and metal free DSSCs.[16] A spacer incorporated between the carbazole donor and an acceptor unit can further increase the molar extinction coefficient of these systems.[17] For the dyes reported here, a squaraine moiety is used as a spacer between the carbazole thiophene donor and indolium acceptor thereby reaching molar absorptivities better than metal complex dyes.

The parent squaraine dye CTSQ-2 co-sensitized with triphenylamine dye (TPD) was reported by Gräf *et al.* in 2013 for application in solid state DSSC which gave an efficiency of 2.43% using spiro-OMeTAD as the hole transporting material.[18] CTSQ-2 with excited state much close to TiO_2 conduction band leaves little driving force for electron injection in DSSC (Scheme 2). Surprisingly a slight modification of the peripheral carbazole by removing the *tertiary* butyl groups increased driving force by 90 mV for the novel CTSQ-1 dye giving an overall better performance in comparison to CTSQ-2. The effect of electron injection was monitored using current-voltage (J-V), incident photon-to-current conversion efficiency (IPCE), lifetime and electrochemical impedance spectroscopy (EIS) measurements through judicious modulation of the conduction band edge by having various Li^+ concentration in the electrolyte. Increased Li^+ concentration will result in a downward shifting of TiO_2 conduction band edge resulting in better injection and decreased open-circuit voltage.[19] Theoretical calculations were carried out to have a detailed understanding of the ground and excited state electron density distribution. To the best of our knowledge, this is the first report on the application of carbazole thiophene donor appended unsymmetrical squaraine dyes in liquid state dye-sensitized solar cells.

2. Experimental

2.1. Materials and Instruments

The precursor chemicals, carbazole, 2-bromothiophene and (±)-trans-1,2-diaminocyclohexane and squaric acid were purchased from Sigma-Aldrich. 4-Hydrazinobenzoic acid and 3-methyl-2-butanone were purchased from Alfa-Aesar. Synthesis of CTSQ-2 was carried out based on previous literature report[18] and the characterization details were given in supporting information. Silica gel used for column chromatography (100-200 mesh size)

was purchased from Merck. All the solvents and reagents were dried and purified by standard methods. The ^1H-NMR and ^{13}C-NMR (500 MHz) were taken using Bruker Advance DPX spectrometer with trimethylsilane (TMS) as internal standard. All the mass spectra containing (M+1) peak were done by ESI technique under Thermo Scientific EXACTIVE spectrometer. Absorption spectra were taken in 1.0 cm width quartz cell using Shimadzu UV-3101 PC UV-vis-NIR spectrophotometer and emission spectra were taken in 1.0 cm width quartz cell using PerkinElmer spectrofluorimeter. Electrochemical measurements were done at a scanning rate of 100 mVs^{-1}, equipped with a normal one compartment cell with glassy carbon working electrode, Pt counter electrode, and Ag/AgCl reference electrode. The measurements were performed in dichloromethane (DCM) solution containing 0.1 M tetrabutylammonium hexafluorophosphate (TBAPF$_6$) as supporting electrolyte. Lifetime measurements were carried out using IBH TCSPC (Time Correlated Single Photon Counting) instrument.

Scheme 1. Synthetic methodology and structure of CTSQ-1 and CTSQ-2
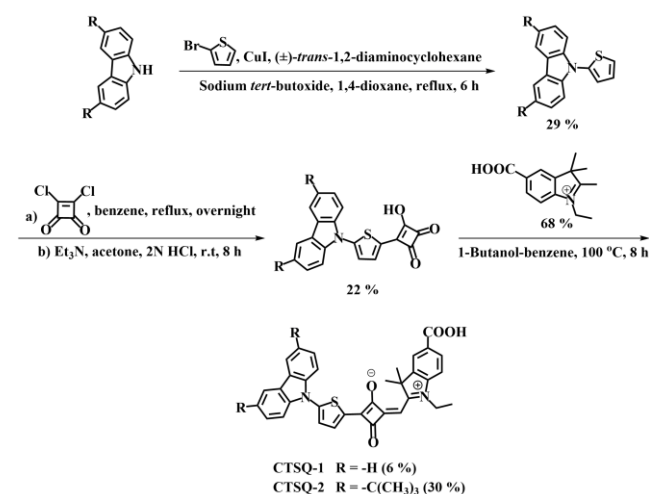
2.2. Synthesis

2.2.1. Synthesis of 9-(thiophene-2yl)-9*H*-carbazole

9*H*-Carbazole (10 g, 60 mmol), 2-bromothiophene (11.3 mL, 120 mmol), (±)-trans-1,2-diaminocyclohexane (17.9 mL, 15 mmol), Sodium *tert*-butoxide (8.6 g, 89.7 mmol) and CuI (2.8 g, 15 mmol) were dissolved in 1,4-dioxane (150 mL). The reaction mixture was refluxed for 6 h. The solvent was removed under reduced pressure and the crude mixture subjected to silica gel (100-200 mesh) column chromatography using 5% chloroform in hexane as eluent to get the pure product (4.65 g, 29%). ^1H-NMR (500 MHz, CDCl$_3$, TMS): δ 8.02 (d, J = 8 Hz, 3H), 7.37 (q, 4H), 7.31 (d, J = 3 Hz, 1H), 7.23 (d, J = 1.5 Hz, 2H), 7.12 (q, 2H) ppm. ESI-MS (m/z): [M+] calcd. for $C_{16}H_{11}NS$: 249.06; found: 250 [M+1].

2.2.2. Synthesis of semisquaraine

9-(thiophen-2-yl)-9*H*-carbazole (12.6 g, 50 mmol) and squaryl chloride (6.1 g, 40 mmol) were dissolved in dry benzene (50 mL) and the reaction mixture was refluxed under argon atmosphere for overnight. The solvent was removed under reduced pressure and residue was subjected to a fast silica gel (100-200 mesh)

column chromatography using 20% chloroform:hexane as the eluent. The product thus obtained was dissolved in dry acetone (50 mL) and triethylamine (6 mL) and put for stirring under argon atmosphere at room temperature for 5 h. The solvents were removed under reduced pressure and the residue obtained was reacted with 2N HCl (50 mL) for 3 h resulting in the formation of a red precipitate which was filtered and dried (3.7 g, 22%). ESI-MS (*m/z*): [M+] calcd. for $C_{20}H_{11}NO_3S$: 345.05; found: 346.05 [M+].

2.2.3. Synthesis of 2,3,3-trimethyl-3*H*-indole-5-carboxylic acid

Glacial acetic acid (15 mL) was added to a mixture of 4-hydrazinobenzoic acid (1.0 g, 6.6 mmol), 3-methyl-2-butanone (1.1 mL, 9.9 mmol) and sodium acetate (1.1 g, 13.2 mmol) and the brown suspension thus obtained was refluxed for 8 h. The solvent was removed under reduced pressure and the residue resulted was redissolved into a clear solution using water and methanol (9:1). Insoluble material was filtered off and the filtrate was allowed to stand at room temperature. The crystals of 2,3,3-trimethyl-3H-indole-5-carboxylic acid (0.94 g, 70%) were collected by filtration.^{1}H-NMR (500 MHz, CD$_3$OD, TMS): δ 1.37 (s, 6H), 2.35 (s, 3H), 7.50 (d, J = 10 Hz, 1H), 8.0 (m, 2H) ppm. ESI-MS (*m/z*): [M+] calcd. for $C_{12}H_{13}NO_2$: 203.24; found: 204.10 [M+1].

2.2.4. Synthesis of 5-carboxy-1-ethyl-2,3,3-trimethyl-3*H*-indol-1-ium

2,3,3-trimethyl-3*H*-indole-5-carboxylic acid (1.0 g, 4.9 mmol) and iodoethane (1.1 g , 7.4 mmol) were dissolved in acetonitrile (25 mL) and refluxed under argon for 10 h. The solvent was removed under reduced pressure and the crude product was washed three times with diethyl ether and air dried (0.78 g, 68%). ^{1}H-NMR (500 MHz, DMSO-*d*$_6$, TMS): δ 1.53 (t, J = 10 Hz, 3H), 1.57 (s, 6H), 2.87 (s, 3H), 4.45 (q, 2H), 8.07 (d, J = 8 Hz, 1H), 8.15 (d, J = 8 Hz, 1H), 8.38 (s, 1H) ppm. ESI-MS (*m/z*): [M+] calcd. for $C_{14}H_{18}NO_2^+$: 232.13: found 232.133 [M+].

2.2.5. Synthesis of CTSQ-1

The semisquaraine (0.57 mg, 1.66 mmol) and indolium cation (0.39 mg, 1.66 mmol) were dissolved in benzene-butanol solvent mixture (1:1) and stirred well at 100 °C for 8 h. Solvents were removed under reduced pressure and pure compound was separated by silica gel (100-200 mesh) column chromatography using 5% MeOH:DCM as eluent (40 mg, 6.1%). ^{1}H-NMR (500 MHz, CDCl$_3$, TMS): δ 1.54-1.54 (t, J = 2.5 Hz, 3H), 1.87 (s, 6H), 4.37-4.39 (q, 2H), 6.48 (s, 1H), 7.31-7.35 (m, 3H), 7.40-7.41 (s, 1H), 7.46-7.48 (m, 2H), 7.74-7.76 (m, 2H), 8.10-8.11 (m, 3H), 8.19 (s, 2H) ppm. ^{13}C-NMR (125 MHz, CDCl$_3$, TMS): δ 12.81, 25.94, 40.65, 51.46, 92.01, 110.71, 111.47, 120.39, 121.6, 124.27, 124.45, 124.69, 126.69, 127.27, 130.85, 131.17, 140.72, 143.40, 144.05, 146.75, 178.51, 178.57, 182.75 ppm. ESI-MS (*m/z*): [M+] calcd. for $C_{34}H_{26}N_2O_4S$: 558.16; found: 559.17 [M+1]. Elemental Analysis for $C_{34}H_{26}N_2O_4S$: C, 73.10; H, 4.69; N, 5.01. Found: C, 73.26; H, 4.67; N, 5.08.

2.3. Fabrication and Characterization of DSSC

The FTO obtained from Dyesol were prepared for TiO$_2$ deposition by stepwise cleaning procedure using detergent, distilled water, acetone and isopropanol by sonication and finally by UV-O$_3$ treatment and TiCl$_4$ deposition which was done by immersing electrodes into a 40 mM TiCl$_4$ aqueous solution at 70 °C for 30 min and then washed with distilled water and ethanol. The photoanodes were then annealed at 500 °C for 30 min. After cooling, transparent TiO$_2$ paste having particle size of 20 nm was deposited followed by annealing at 125 °C for 10 min. TiO$_2$ paste consisting larger TiO$_2$ particles (ca. 400 nm, Dyesol) was coated on top of the first layer and annealed at 125 °C for 10 min. This was followed again by TiCl$_4$ treatment and annealing. The electrodes were then put into programmed heating at 325 °C for 15 min, 450 °C for 15 min, and 500 °C for 30 min and slowly cooled down to room temperature and electrodes were immersed into squaraine dye solution in CHCl$_3$/MeOH (1:1) mixture with chenodeoxycholic acid (CDCA) (10 mM) and kept at room temperature for 15 h. Counter electrodes were prepared by coating with a drop of H$_2$PtCl$_6$ solution (2 mg of Pt in 1mL ethanol) on FTO plates having pre-drilled holes and cleaned using the same procedure as for photoanodes, the only difference being washing done by using acidified ethanol (0.1 N HCl in ethanol). The dye adsorbed TiO$_2$ electrodes and Pt counter electrodes were assembled with hot press using 25 μm surlyn spacer. The space in between both the electrodes were filled with liquid I^-/I_3^- electrolyte which was composed of various compositions of 1-butyl-3-methylimidazolium iodide (BMII), lithium iodide (LiI), iodine (I$_2$), guanidinium thiocyanate (GuSCN) and 4-*tert*-butyl pyridine (tbp) in acetonitrile. The drilled holes were sealed with microscopic cover slide and surlyn to avoid electrolyte leakage. Three cells were fabricated for each condition and the cells were measured after keeping it for 12 h in dark.

The photovoltaic performance of the fabricated DSSC were measured using an AM 1.5 solar simulator (Newport Instruments, USA) equipped with a source meter (Keithley 2400) at 25 °C. The IPCE measurement of the devices was performed under DC mode using a 250W xenon lamp coupled with Newport monochromator. A monochromatic beam was continuously irradiating on the sample and the current was measured using Keithley 6430 source meter. NIST calibrated Si photodiode was used to find the incident power spectral response of the light. The J-V properties of cells were measured using square shade mask with active area 0.25 cm^2 (without mask active area is 0.36 cm^2). The power of the simulated sunlight was calibrated by using a reference Si photodiode supplied by Newport instruments. Open circuit voltage (V_{oc}) decay measurements are done at open circuit. The cell was in the dark at the beginning of the measurement, and then the lights were turned on until the voltage got stabilized, followed by switching the light off and recording the decay of photovoltage. Lifetime data was transformed from the voltage decay part of the measurement through previously reported methods.[20] The EIS measurements of DSSC were carried out using a micro Autolab (μ3AUT70904) equipped with FRA mode under forward bias in the dark. The measurements were performed in a frequency range of 0.1 to 10^5 Hz with ac amplitude of 10 mV.

3. Results and Discussion

3.1.   Design and Synthesis

The synthetic details with molecular structures for both squaraine sensitizers (CTSQ-1 and CTSQ-2) are represented in Scheme 1. In order to facilitate efficient electron injection to the conduction band of TiO$_2$ and to have a better adsorption on the semiconductor surface both squaraine dyes were designed in such a way to have carboxyl group positioned on indolium acceptor part. Even though carbazole was used as an efficient electron donor in metal-free organic dyes and metal complex dyes,[21,22] their use as a suitable donor in unsymmetrical squaraine sensitizers for DSSCs has not been much explored. So we designed and synthesized two unsymmetrical squaraine dyes appended with carbazole thiophene (CTSQ-1) and substituted carbazole thiophene with electron donating *tertiary* butyl groups on the peripheral carbazole unit (CTSQ-2) for application in dye-sensitized solar cells. In both these dyes carbazole linked thiophene unit functioned as the electron donor component whereas *N*-carboxyethyl quarternized indolium moiety acted as the electron acceptor part. The chemical structure of CTSQ-1 and CTSQ-2 differ only in their substitution at the 3,6 positions of the carbazole moiety.

For the synthesis of CTSQ-1, initially, carbazole and 2-bromothiophene were made to undergo C-N coupling reaction using (±)-trans-1,2-diaminocyclohexane and CuI as catalyst in 1,4-dioxane to form 9-(thiophene-2yl)-9*H*-carbazole. Squarylium chloride was synthesized by refluxing squaric acid with thionyl chloride in benzene and a catalytic amount of DMF. The C-N coupled product 9-(thiophene-2yl)-9*H*-carbazole was made to react with squarylium chloride in presence of benzene for 6 h resulting in the formation of semisquaryl chloride, which was followed by hydrolysis using triethylamine and 2N HCl to form semisquaraine. The second precursor for squaraine (5-Carboxy-2,3,3-trimethyl-1-ethyl-3H-indolium iodide) was prepared by Fisher Indole synthesis using *p*-phenyl hydrazine benzoic acid and isopropyl ketone in presence of glacial acetic acid using sodium acetate as a base to form 2,3,3-trimethyl-2,3-dihydro-1*H*-indole-5-carboxylic acid. Indole acid, thus obtained was alkylated by treatment with ethyl iodide in the presence of dry acetonitrile to form 5-carboxy-1-ethyl-2,3,3-trimethyl-3*H*-indolium. Squaraine reaction was then carried out by condensation between carbazole thiophene semisquaraine and alkylated indolium acid using benzene/butanol (1:1) mixture to form CTSQ-1. For CTSQ-2 the procedure followed was exactly same as that of CTSQ-1, the only difference being Friedel-Crafts alkylation carried out in order to substitute the peripheral carbazole ligand with *tertiary* butyl groups. The squaraine dyes formed were purified by column chromatography using 3% methanol/dichloromethane mixture couple of times until the squaraine dyes are completely pure. Each step of the above reactions was fully characterized using ^{1}H NMR, ^{13}C NMR and mass data (Fig. S9-S17, SI).

3.2.   Photophysical Properties

The absorption spectra of CTSQ-1 and CTSQ-2 in CH$_2$Cl$_2$ solution are shown in Figure 1(a), and the characteristic data are summarized in Table 1. Both the dyes exhibited intense and sharp absorption in the visible-NIR region ranging from 500-700 nm.

For CTSQ-1 and CTSQ-2, the absorption maxima in DCM were found at 605 nm (ε = 31800 M^{-1} cm^{-1}) and 637 nm (ε =56858 M^{-1}cm^{-1}) respectively. The red-shift in the absorption spectra of CTSQ-2 in comparison to CTSQ-1 happens since the electron donating tertiary butyl groups on the peripheral carbazole donor stabilizes the lowest unoccupied molecular orbital (LUMO) thereby reducing the energy gap.[12] The absorption spectra of both squaraine sensitizers in solution and on TiO$_2$ film are compared in Figure 1(b). The absorption spectra of both dyes on TiO$_2$ electrodes are broad which clearly shows the increased interaction between the dyes and TiO$_2$. It is quite apparent from Figure 1(b) that there is a blue-shift in the absorption maxima which is mainly due to the deprotonation between carboxylic acid and TiO$_2$ semiconductor.[23] The dyes exhibited fluorescence emission at 666 nm for CTSQ-1 and 688 nm for CTSQ-2 in DCM (Fig. S3, SI). Lifetime decay plots for CTSQ-1 and CTSQ-2 in DCM are given in Fig. S6 (SI).
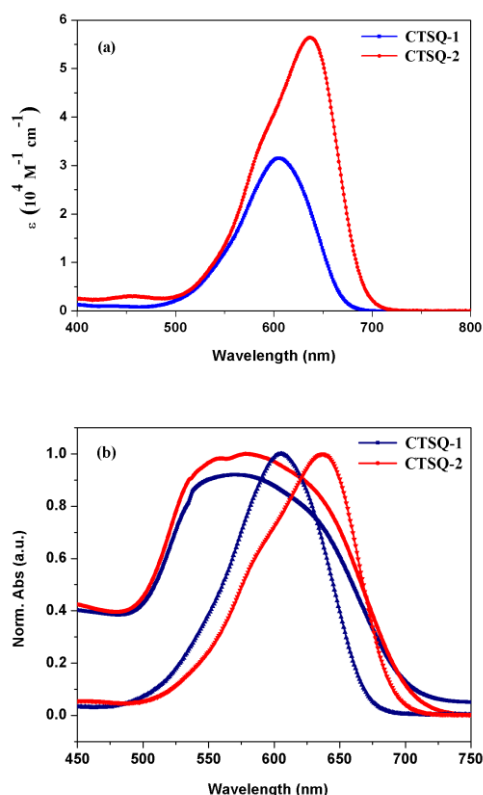

Figure 1. (a) Absorption spectra of CTSQ-1 and CTSQ-2 plotted against molar absorption coefficient in DCM as solvent (Conc. 1×10^{-5}M); (b) normalized absorption spectra of CTSQ-1 and CTSQ-2 on TiO$_2$ in comparison with the normalized absorption spectra of dyes in DCM.

3.3.   Electrochemical Properties

The electrochemical properties were investigated using cyclic voltammetry (CV) and square wave voltammetry in order to gain more understanding on ground and excited state potentials of CTSQ-1 and CTSQ-2 sensitizers and to evaluate the possibility of photoelectron injection into the conduction band of TiO$_2$ and regeneration of oxidized ground state of squaraine dyes by the electrolyte (Fig. S4, S5, SI). The measurements were performed

in DCM solution at a scan rate of 100 mVs^{-1} using Ag/AgCl reference electrode that was calibrated with ferrocene. All the potentials measured were converted to NHE considering Fc/Fc$^+$ as +0.765 V *vs.* NHE in DCM.[24] To bring about efficient charge separation, the ground state oxidation potential of dyes should be more positive than the redox potential of the I$^-$/I$_3^-$ electrolyte (0.40 V *vs.* NHE) to have efficient regeneration, and excited state oxidation potential of dyes should be more negative than the conduction band edge of TiO$_2$, E$_{cb}$ (-0.5 V *vs.* NHE) to have efficient injection.[25] The ground state oxidation potentials E$_{ox}$ correspond to the HOMO levels and were respectively 1.19 V and 1.21 V for CTSQ-1 and CTSQ-2 (Table 1). The excited state oxidation potentials can be calculated from the values of ground state oxidation potential and the zero-zero band gaps (E$_{0-0}$) determined by the intersection of absorption and emission spectra in DCM (Fig. S1, S2, SI). The estimated E$_{0-0}$ is 1.93 V and 1.86 V for CTSQ-1 and CTSQ-2 respectively. Subsequently the excited state oxidation potentials for CTSQ-1 and CTSQ-2 calculated from E$_{ox}$ - E$_{0-0}$ are -0.74 V and -0.65 V *vs.* NHE respectively. The excited state levels were only slightly more negative than conduction band edge of TiO$_2$ (-0.5 V *vs.* NHE) resulting in a diminished driving force for electron injection from the excited state of squaraine dyes into the conduction band of TiO$_2$.

Table 1. Photophysical and electrochemical characteristics of CTSQ-1 and CTSQ-2.

Dye	λ$_{max}$/nm[a]	ε/M^{-1}cm^{-1}[a]	λ$_{em}$/nm[a]	τ/ns[a]	HOMO/V (V vs NHE)[b]	E$_{0-0}$/V eV[c]	LUMO/V (V vs NHE)[d]
CTSQ-1	605	3.15 × 10^4	666	0.63	1.19	1.93	-0.74
CTSQ-2	637	5.64 × 10^4	688	1.43	1.21	1.86	-0.65

[a]Measured in DCM. [b]The oxidation potential was measured using 0.1 M TBAPF$_6$ in DCM. [c]Estimated from the intersection of absorption and emission spectra in DCM. [d]Calculated using the equation HOMO-E$_{0-0}$

Scheme 2. Ground and excited state energy levels of CTSQ-1 and CTSQ-2 sensitizers (Potential *vs.* NHE)
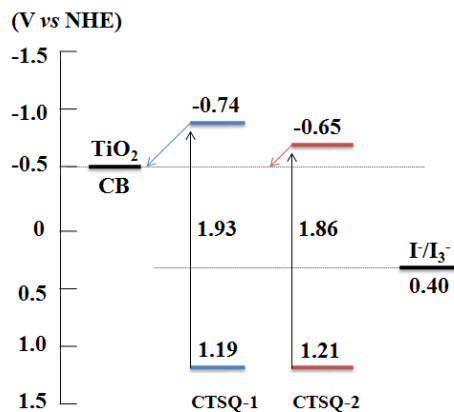
3.4. Theoretical Calculations

To have a deeper insight regarding the geometrical structures and electronic properties of CTSQ-1 and CTSQ-2, density functional theory (DFT) calculations were performed at the M06/6-311G (d,p) level using Gaussian 09 program.[26] The electron distribution of both HOMO and LUMO levels are given in Figure 2. The HOMO for both CTSQ-1 and CTSQ-2 are delocalized over the carbazole thiophene and central cyclobutene core whereas the LUMO orbitals are distributed over the thiophene ring, cyclobutene core and indolium acceptor unit. The charge transfer in both CTSQ-1 and CTSQ-2 is less efficient since the electron density in LUMO for both dyes are not concentrated on the acceptor part but distributed over a wider range of π-spacer. For efficient electron injection to happen from the excited state dyes to the conduction band of TiO$_2$, the LUMOs should be distributed as close as to the anchoring groups in order to have efficient overlap with the titanium 3d orbitals that will instigate electron injection.[27] The optimized geometry with bond lengths are given in supporting information (Fig. S8, SI). CTSQ-2 with electron donating *t*-butyl groups resulted in a decrease of carbazole thiophene bond length. The dihedral angles between the carbazole and thiophene units are quite similar for both the dyes with 50° for CTSQ-1 and 47° for CTSQ-2 while the rest of the π–conjugated portion of the dye is coplanar. This suggests that both CTSQ-1 and CTSQ-2 possess similar geometrical features, and the carbazole moiety is mainly responsible for maintaining an overall non-planar geometry of these dyes.
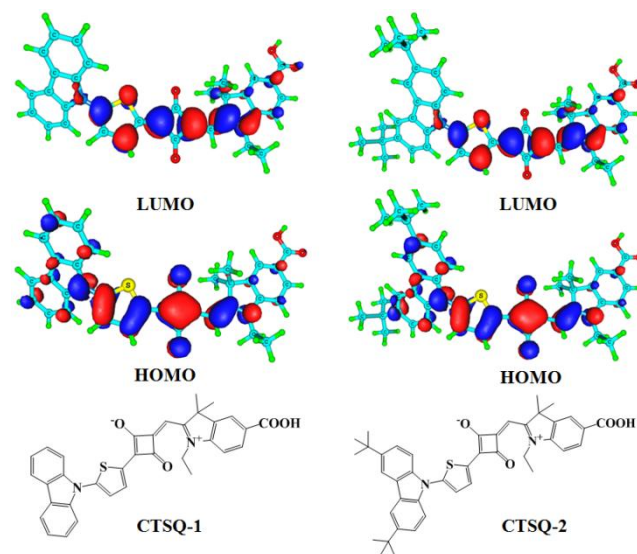

Figure 2. DFT calculations performed at the M06/6-311G (d,p) level depicts the frontier molecular orbitals electron density picture of the squaraine sensitizers.

3.5. Solar Cell Performance

The photovoltaic properties consisting of short-circuit current density (J$_{sc}$), open-circuit photovoltage (V$_{oc}$), fill factor (FF) and total power conversion efficiency (µ) of solar cells fabricated with TiO$_2$ photoelectrodes sensitized with CTSQ-1 and CTSQ-2 having I$^-$/I$_3^-$ as electrolyte is summarized in Table 2. The J-V characteristics and IPCE spectra for devices are illustrated in Figures 3(a) and 3(b) respectively. Under the same fabrication conditions DSSCs based on CTSQ-1 showed the highest power conversion efficiency (PCE) of 2.94% with J$_{sc}$ = 8.42 mAcm^{-2}, V$_{oc}$ = 0.53 V and FF = 0.65 under AM 1.5 irradiation. The CTSQ-

2 sensitized solar cells fabricated under similar conditions with the same electrolyte composition (EL1) displayed a relatively lower photovoltaic efficiency of 2.23% (μ) with J_{sc} = 6.76 mAcm^{-2}, V_{oc} = 0.52 V and FF = 0.64 which is mainly attributed to the lower J_{sc} value. The IPCE spectra also exhibited a similar trend with CTSQ-1 having comparatively better performance than CTSQ-2. It is quite obvious from Scheme 2 that in both the squaraine sensitizers the LUMO levels are placed at potentials much closer to the conduction band edge of TiO$_2$. It is legitimate
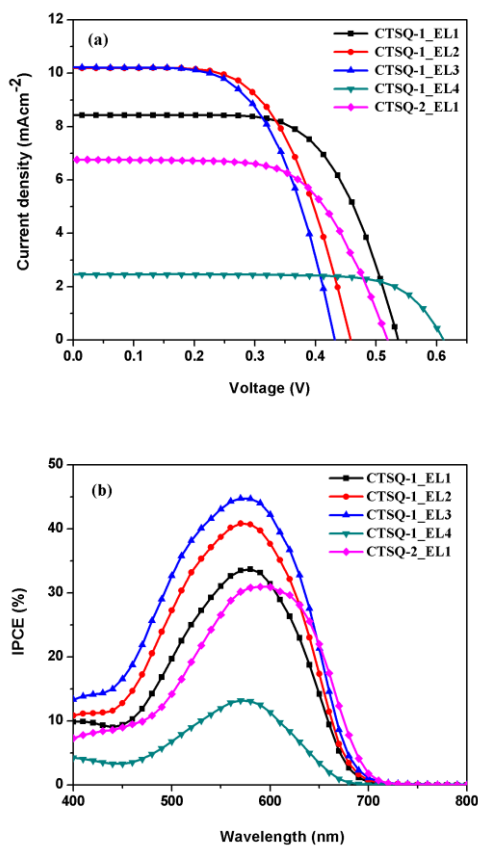

Figure 3. (a) Photocurrentdensity-voltage (J-V) characteristics of DSSCs based on CTSQ-1 and CTSQ-2 under AM 1.5G illumination (100 mWcm^{-2}) (b) Incident photon-to-current conversion efficiency (IPCE) spectra for DSSCs based on CTSQ-1 and CTSQ-2. These data correspond to entries 1-4 and 7 in Table 2.

Table 2. Photovoltaic characteristics of squaraine dyes in a range of electrolyte compositions

Entry	Dye	Electrolyte composition[a]	J_{sc} (mAcm^{-2})	V_{oc} (V)	FF	μ (%)
1	CTSQ-1	EL1	8.42	0.53	0.65	2.94
2	CTSQ-1	EL2	10.19	0.45	0.60	2.80
3	CTSQ-1	EL3	10.21	0.43	0.59	2.63
4	CTSQ-1	EL4	2.45	0.61	0.74	1.11
5	CTSQ-1	EL5	1.87	0.55	0.69	0.70
6	CTSQ-1[b]	EL1	5.90	0.52	0.68	2.11
7	CTSQ-2	EL1	6.76	0.52	0.64	2.23

Condition: dye concentration (0.1 mM), CDCA concentration (10 mM); photoelectrode, TiO$_2$ film thickness is active (11.5 μm) and scattering layer (3.5 μm). 0.25 cm^2 active area using mask. [a]Electrolyte composition, EL1 - 0.6 M BMII, 0.03 M I$_2$, 0.1 M LiI; EL2 - 0.6 M BMII, 0.03 M I$_2$, 0.5 M LiI; EL3 - 0.6 M BMII, 0.03 M I$_2$, 1 M LiI; EL4 - 0.6 M BMII, 0.03 M I$_2$, 0.05 M LiI, 0.05 M GuSCN, 0.25 M tbp; EL5 - electrolyte from dyesol. [b] Dye concentration used is 0.05 mM

that the injection of excited electrons from the sensitizers to the conduction band of TiO$_2$ is expected to be incompetent leading to lower IPCE maxima for both CTSQ-1 and CTSQ-2. Out of which CTSQ-1 having the LUMO positioned 90 mV more negative to CTSQ-2 exhibited better current density and IPCE performance that is justifiable based on increased driving force for electron injection.

In liquid state DSSC, Li salts are usually added to have a tunability of Fermi level in a way to enhance the injection driving force.[28,29] The effect of electron injection is followed in detail for CTSQ-1 by varying the Li$^+$ concentration in electrolyte. As the concentration of Li$^+$ in electrolyte increases that will tentatively push the conduction band edge more positive leading to enhanced driving force for electron injection as reported by O'Regan and Durrant which will ultimately result in getting a better current density and IPCE profile.[30] As shown in Figure 3(a), when we systematically increased the Li$^+$ concentration from 0.1 M to 1 M the current density got elevated from 8.42 mAcm^{-2} to 10.21 mAcm^{-2}, but the net efficiency decreased as a result of voltage drop since photovoltage is measured as the difference of Nernst potential of the electrolyte and Fermi level of semiconductor later which is pushed more positive by higher Li$^+$ concentration resulting in voltage drop. The IPCE data obtained (Fig. 3b) also complimented this argument.

The IPCE can be expressed in terms of light harvesting efficiency (LHE), electron injection efficiency (Φ_{ing}), regeneration efficiency (η_{reg}) and charge collection efficiency (η_{cc}) as given by equation (1).

$$IPCE (\lambda) = LHE (\lambda) \times \Phi_{ing} \times \eta_{reg} \times \eta_{cc} \qquad (1)$$

For entries 1 to 3 in Table 2, by having same dye (CTSQ-1), same semiconductor (TiO$_2$) and same electrolyte (I$^-$/I$_3^-$) we can assume that the LHE, η_{reg} and η_{cc} to be unity. The change of IPCE

can thus be tracked directly to the change in injection driving force which is modulated by pushing the conduction band edge more positive by having more Li^+ concentration in the electrolyte. From the IPCE spectra given in figure 3(b), it is visible that as we

5 change the electrolyte from EL1 to EL3 the IPCE maximum increased by almost 10-15%. This shows that even though CTSQ-2 has a better absorption profile in comparison to CTSQ-1, the former dye is injection limited which ultimately resulted in a lower photovoltaic performance.

10

The IPCE spectra with varying amounts of LiI displayed that as the concentration of Li^+ increases there is more broadening of the spectra at the higher energy region that might be due to the formation of H-aggregates as observed in solution state with

15 similar kind of systems.[18] H-aggregation involves a plane to plane alignment that is dominated by molecules having less steric effects.[31,32] More detailed insight into the effect of aggregation on photovoltaic parameters is outside the scope of the current paper and will be reported in detail elsewhere. State of the art squaraine

20 sensitizers reported by Grätzel *et al.*[33] used an electrolyte composition given as EL4 having only 0.05 M LiI and 0.25 M tbp. The presence of tbp resulted in shifting the conduction band edge to more negative potentials[34] thereby impeding electron injection from CTSQ-1 to the semiconductor ensuing lesser

25 current density and lower IPCE values (entry 4 in Table 2). Commercial electrolyte from Dyesol (EL5) was used for comparison (entry 5 in Table 2) which gave very poor performance in comparison to homemade electrolytes with the squaraine sensitizers which might be due to the presence of

30 excess tbp as explained for EL4 (Fig. S7, SI). Since squaraine sensitizers are reported to exhibit aggregation at higher concentration[12,18] we fabricated devices with CTSQ-1 where the concentration of the dye solution was taken to be 0.05 M (entry 6 in Table 2), half the concentration of that of the best performing

35 devices using the electrolyte composition EL1 which resulted in a J_{sc} of 5.90 mAcm^{-2}, V_{oc} of 0.52 V, FF of 0.68 and a net efficiency of 2.11% which is less than the performance of devices fabricated under similar conditions using 0.1 M of the dye solution (entry 1 in Table 2) which is attributed to lesser dye loading (Fig. S7, SI).

40 This shows that aggregation is not playing significant roles in the photovoltaic performance of solar cells fabricated using CTSQ-1 and CTSQ-2 sensitizers.
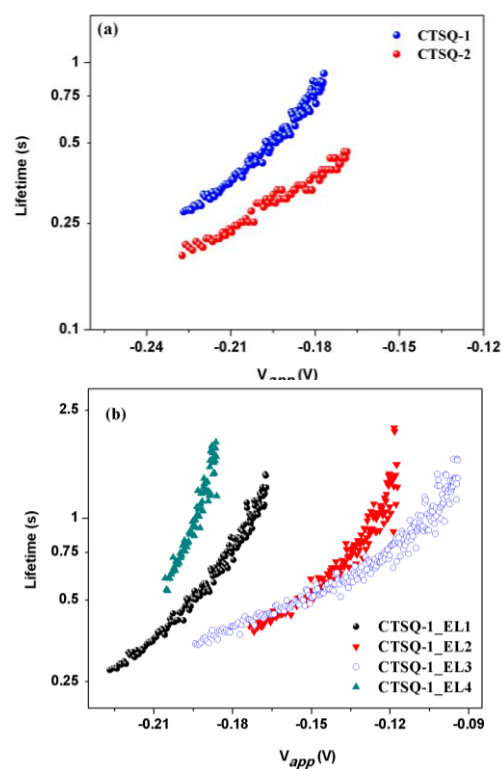

45 **Figure 4.** Electron lifetime plots of squaraine dyes as a function of open circuit voltage (a) comparison of CTSQ-1 and CTSQ-2 (b) lifetime in four different electrolytes with varying Li^+ concentration carried out using charge extraction method.

50 The electron lifetime plots for both CTSQ-1 and CTSQ-2 are given in Figure 4(a). CTSQ-2 with peripheral *t*-butyl groups was expected to prevent recombination to a better extent than CTSQ-1, but the results obtained (Fig. 4a) displayed better lifetime for CTSQ-1 in comparison to CTSQ-2. CTSQ-1 with a higher

55 LUMO level resulted in better injection thereby preventing recombination and having a better lifetime.

Figure 4(b) shows the electron lifetime plots for CTSQ-1 in four different electrolytes with variable Li^+ additive compositions. It is

60 discussed already from J-V and IPCE data (Fig. 3) that increasing the concentration of Li^+ in electrolyte will result in shifting of conduction band edge more positive thereby improving the driving force for electron injection. This shift of conduction band edge and surface states closer to the redox potential of electrolyte

65 leads to more recombinations and reduced lifetime for devices having higher Li^+ concentration. Kopidakis *et al*. had already reported that intercalation of Li^+ into the nanocrystalline TiO_2 will result in increased charge recombinations thereby resulting in decreased lifetime.[35] The lifetime shown in Figure 4(b) decreased

70 in the order EL3<EL2<EL1. This is also supported by the drop in photovoltage on moving from EL1 to EL3. For devices fabricated with higher tbp concentration (EL4, entry 4 in Table 2) conduction band edge was displaced to more negative potentials thereby preventing recombinations resulting in better lifetime and
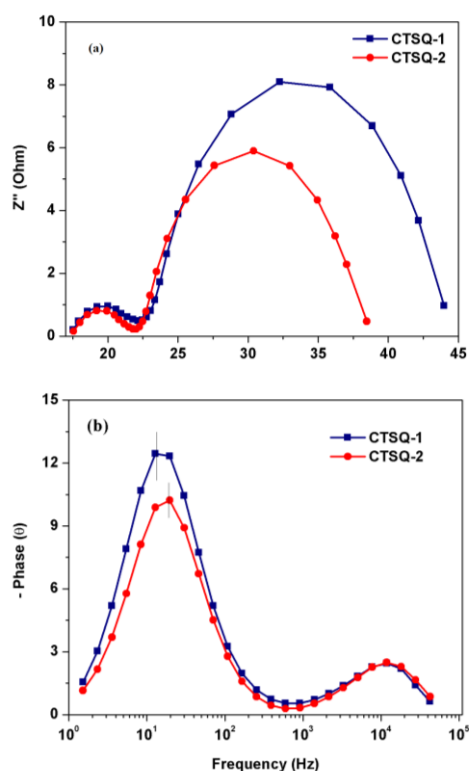
75 photovoltage.

Figure 5. EIS spectra of DSSCs based on CTSQ-1 and CTSQ-2 measured at -0.65 V forward bias in the dark (a) Nyquist, and (b) Bode phase plots.

EIS analysis of CTSQ-1 and CTSQ-2 sensitized DSSCs were performed in order to elucidate the interfacial charge recombination process in DSSC based on these dyes under dark condition.[36] As shown in Figure 5(a) the major semicircle for each dye in the EIS Nyquist plot corresponds to the resistance of electron transport at the TiO_2/dye/electrolyte interface which implies the resistance of recombination between electrons in TiO_2 conduction band and oxidized I_3^- species in electrolyte.[37,38] The larger the semicircle, slower the recombination kinetics. It is evident from the Nyquist plot that CTSQ-2 even with terminal *tertiary* butyl groups exhibited lesser recombination resistance that is most likely due to the lower driving force for electron injection. This trend is consistent with the lifetime plots and V_{oc} values of the cells. In bode plots, (Fig. 5b) the peaks at middle frequency are associated with the charge transfer resistances at the TiO_2/dye/electrolyte interface.[39] The electron lifetime are correlated with the reciprocal of the peak frequency for middle-frequency peaks.[40] The peak for CTSQ-2 is right shifted compared to CTSQ-1 exhibiting a lower electron lifetime. Overall, based on the above results we believe that carbazole thiophene can be used as an efficient donor for unsymmetrical squaraine dyes but its excited state energetics need to be modified in such a way to have enough driving force for electron injection. This leaves further space for improvement by having more electron withdrawing units at the peripheral carbazole group. Detailed investigation of injection kinetics using femtosecond laser along with studies on the effect of Li^+ concentration on electron diffusion length and TiO_2 band gap state distribution using EIS measurements are currently under investigation.

4.　　Conclusion

In conclusion, we have synthesized two unsymmetrical squaraine sensitizers incorporating carbazole thiophene (CTSQ-1) and *t*-butyl substituted carbazole thiophene (CTSQ-2) as electron donor units linked to indolium acceptor and applied in DSSCs. It has been demonstrated that we can readily tune the LUMO energy levels of these unsymmetrical squaraine sensitizers by modifying the substituent on the peripheral carbazole unit. Both CTSQ-1 and CTSQ-2 exhibited intense absorption in the visible-NIR region. Best devices gave a power conversion efficiency of 2.94% for CTSQ-1 and 2.23% for CTSQ-2 sensitized solar cells using I^-/I_3^- redox electrolyte. Even though carbazole thiophene is an excellent donor unsymmetrical squaraine sensitizers having this donor resulted in lack of enough driving force for electron injection. A mere modification of the peripheral carbazole unit helped in improving the injection driving force. CTSQ-1 with better excited state energetics is having higher injection driving force and is more successful in preventing recombinations compared to CTSQ-2, which is evident from lifetime and EIS measurements leading to better solar cell performance for CTSQ-1 in couple to CTSQ-2. Even though CTSQ-1 performed better than CTSQ-2 the lack of excited state electron density distribution near to the anchoring group coupled with lack of enough driving force for electron injection resulted in efficiencies lower than that of state of the art unsymmetrical squaraine dyes.

References

1　H. B. Gray, *Nature Chemistry.*, 2009, **1**, 7.
2　M. G. Walter, E. L. Warren, J. R. McKone, S. W. Boettcher, Q. Mi, E. A. Santori, and N. S. Lewis, *Chem. Rev.*, 2010, **110**, 6446.
3　M. Grätzel, *Acc. Chem. Res.,* 1981, **14**, 376; (b) J. A. Turner, *Science.,* 2004, **305**, 972; (c) N. S. Lewis. *Science.,* 2007, **315**, 798.
4　L. Han, A. Islam, H. Chen, C. Malapaka, B. Chiranjeevi, S. Zhang, X. Yang and M. Yanagida, *Energy Environ. Sci.*, 2012, **5**, 6057.
5　The U.S. Photovoltaic Industry Roadmap, *http://www.nrel.gov/docs/gen/fy03/30150.pdf* (accessed May 2, 2015)
6　B. O. Regan and M. Grätzel, *Nature.*, 1991, **353**, 737.
7　A. Hagfeldt and M.Grätzel, *Acc. Chem. Res.*, 2000, **33**, 269.

8   J. Yum, E. Baranoff, S. Wenger, Md. K. Nazeeruddin and M. Grätzel, *Energy Environ. Sci.*, 2011, **4**, 842.

9   (a) Md. K. Nazeeruddin, S. M. Zakeeruddin, R. H-Baker, M. Jirousek, P. Liska, N. Vlachopoulos, V. Shklover, C-H. Fischer and M. Grätzel, *Inorg. Chem.*, 1999, **38**, 6298; (b) T. Kinoshita, J-i. Fujisawa, J. Nakazaki, S. Uchida, T. Kubo and H. Segawa, *J. Phys. Chem.Lett.,* 2012, **3**, 394; (c) L. Han, A. Islam, H. Chen, C. Malapaka, B. Chiranjeevi, S. Zhang, X. Yang and M. Yanagida, *Energy Environ. Sci.,* 2012, **5**, 6057; (d) Y. Numata. S. P. Singh, A. Islam, M. Iwamura, A. Imai, K. Nozaki, and L. Han, *Adv. Funct. Mater.*, 2013, **23**, 1817.

10 (a) M. Grätzel, *Acc. Chem. Res.*, 2009, **42**, 1788; (b) A. Mishra, M. K. Fischer, P. Buerle, *Angew. Chem.*, 2009, **48**, 2474; (c) A. Hagfeldt, G. Boschloo, L. C. Sun, L. Kloo, H. Pettersson, *Chem. Rev.*, 2010, **110**, 6595.

11 S. Mathew, A. Yella, P. Gao, R. H-Baker, B. F. E. Curchod, N. A-Astani, I. Tavernelli, U. Rothlisberger, Md. K. Nazeeruddin and M. Grätzel, *Nature Chemistry.,* 2014, **6**, 242.

12 (a) S. Das, K. G. Thomas, K. J. Thomas, P. V. Kamat and M. V. George, *J. Phys. Chem.,* 1994, **98**, 9291; (b) A. Ajayaghosh,. *Acc. Chem. Res.*, 2005, **38**, 449; (c) E. Arunkumar, A. Ajayaghosh and J. Daub, *J. Am. Chem. Soc.,* 2005, **127**, 3156; (d) S. Sreejith, P. Carol, P. Chithra and A. Ajayaghosh, *J. Mater. Chem.,* 2008, **18**, 264; (e) C. Qin, W-Y. Wong and L. Han, *Chem. Asian J.*, 2013, **8**, 1706.

13 S. Alex, U. Santhosh, S. Das, *J. Photochem. Photobiol. A.*, 2005, **172**, 63.

14 Y. Shi, R. B. Hill, J. H. Yum, A. Dualeh, S. Barlow, M. Grätzel, S. R. Marder and M. K. Nazeeruddin, *Angew. Chem., Int. Ed.,* 2011, **50**, 6619.

15 J. H. Delcamp, Y. Shi, J. H. Yum, T. Sajoto, E. Dell'Orto, S. Barlow, M. K. Nazeeruddin, S. R. Marder and M. Grätzel, *Chem. Eur. J.,* 2013, **19**, 1819.

16 (a) Z-S. Wang, Y. Cui, Y. D-oh, C. Kasada, A. Shinpo and K. Hara, *J. Phys. Chem. C.,* 2008, **112**, 17011; (b) C. J. Chen, J. Y. Liao, Z. G. Chi, B. J. Xu, X. Q. Zhang, D. B. Kuang, Y. Zhang, S. W. Liu and J. R. Xu, *J. Mater. Chem.,* 2012, **22**, 8994; (c) H. Lai, J. Hong, P. Liu, C. Yuan, Y. X. Li and Q. Fang, *RSC Adv.,* 2012, **2**, 2427; (d) G. Marotta, M. A. Reddy, S. P. Singh, A. Islam, L. Han, F. D. Angelis, M. Pastore and M. Chandrasekharam, *ACS Appl. Mater. Interfaces.*, 2013, **5**, 9635.

17 (a) S. Tang, B. Li, and J. Zhang, *J. Phys. Chem. C.*, 2013, **117**, 3221; (b) J. D. Azoulay, Z. A. Koretz, B. M. Wong, and G. C. Bazan, *Macromolecules, 2013.*, **46**, 1337.

18 K. Graf, M. A. Rahim , S. Das, M. Thelakkat, *Dyes and Pigments.*, 2013, **99**, 1101.

19 J. R. Durrant, S. A. Haque and E. Palomares, *Coord. Chem. Rev.*, 2004, **248**, 1247.

20 S. Soman, Y. Xie, T. W. Hamann, *Polyhedron.,* 2014, **82**, 139.

21 (a) C-Y. Chen, J-G. Chen, S-J. Wu, J-Y. Li, C-J. Wu and K-C. Ho, *Angew. Chem. Int. Ed.,* 2008, **47**, 7342; (b) C-Y. Chen, N. Pootrakulchote, S-J. Wu, M. Wang, J-Y. Li, J-H. Tsai, C-J. Wu, S. M. Zakeeruddin and M. Grätzel, *J. Phys. Chem. C.*, 2009, **113**, 20752; (c) S-Q. Fan, C. Kim, B. Fang, K-X. Liao, G-J. Yang, C-J. Li, J-J. Kim and J. Ko, *J. Phys. Chem. C.*, 2011, **115**, 7747; (d) A. El-Shafei, M. Hussain, A. Atiq, A. Islam and L. Han, *J. Mater. Chem.,* 2012, **22**, 24048.

22 A. Venkateswararao, K. R. J. Thomas, C-P. Lee, C-T. Li, and K-C. Ho, *ACS Appl. Mater. Interfaces.*, 2014, **6**, 2528.

23 (a) J. Mao, F. Guo, W. Ying, W. Wu, J. Li, and J. Hua, *Chem. Asian J.*, 2012, **7**, 982; (b) Y. Hua, S. Chang, D. Huang, X. Zhou, X. Zhu, J. Zhao, T. Chen, W-Y. Wong and W-K. Wong, *Chem. Mater.,* 2013, **25**, 2146.

24 K. C. D. Robson, B. Sporinova, B. D. Koivisto, E. Schott, D. G. Brown and C. P. Berlinguette, *Inorg. Chem.*, 2011, **50**, 6019.

25 J. W. Ondersma and T. W. Hamann, *Energy Environ. Sci.*, 2012, **5**, 9476-9480.

26 Y. Zhao and D. G. Truhlar, *J. Chem. Phys.*, 2006, **125**, 194101.

27 D. P. Hagberg, T. Edvinsson, T. Marinado, G. Boschloo, A. Hagfeldt and L. Sun, *Chem. Commun.*, 2006, **21**, 2245.

28 J. R. Jennings and Q. Wang, *J. Phys. Chem*. C, 2010., **114**, 1715.

29 (a) Y. Shi, Y. Wang, M. Zhang and X. Dong, *Phys. Chem. Chem. Phys.*, 2011, **13**, 14590; (b) S. E. B. Koops, B. O'Regan, P. R. F. Barnes and J. R. Durrant, *J. Am. Chem. Soc.*, 2009, **131**, 4808.

30 (a) S. A. Haque, E. Palomares, B. M. Cho, A. N. M. Green, N. Hirata, D. R. Klug, J. R. Durrant, *J. Am. Chem. Soc.,* 2005, **127**, 3456; (b) S. E. Koops, B. C. O'Regan, P. R. F. Barnes, J. R. Durrant, *J. Am. Chem. Soc.,* 2009., **131**, 4808; (c) P. R. F. Barnes, A. Y. Anderson, S. E. Koops, J. R. Durrant, B. C. O'Regan, *J. Phys. Chem. C.*, 2009, **113**, 1126.

31 G. de Miguel, M. Ziółek, M. Zitnan, A. Organero, S. S. Pandey, S. Hayase and A. Douhal, *J. Phys. Chem. C.,* 2012, **116**, 9379.

32 K. Hara, Y. Dan-oh, C. Kasada, Y. Ohga, A. Shinpo, S. Suga, K. Sayama and H. Arakawa, *Langmuir.*, 2004, **20**, 4205.

33 (a) Y. Shi, R. B. Hill, J. H. Yum, A. Dualeh, S. Barlow, M. Grätzel, S. R. Marder and M. K. Nazeeruddin, *Angew. Chem., Int. Ed.,* 2011, **50**, 6619; (b) J. H. Delcamp, Y. Shi, J. H. Yum, T. Sajoto, E. Dell'Orto, S. Barlow, M. K. Nazeeruddin, S. R. Marder and M. Grätzel, *Chem. Eur. J.,* 2013, **19**, 1819.

34 S. Zhang, X. Yang, K. Zhang, H. Chen, M. Yanagida and L. Han, *Phys. Chem. Chem. Phys.,* 2011, **13**, 19310.

35 N. Kopidakis, K. D. Benkstein, J. van de Lagemaat, A. J. Frank, *J. Phys. Chem. B.*, 2003, **107**, 11307.

36 (a) Q. Wang, J-E. Moser, and M. Gratzel *J. Phys. Chem. B.,* 2005, **109**, 14945; (b) G. Wu, F. Kong, Y. Zhang, X. Zhang, J. Li, W. Chen, W. Liu, Y. Ding, C. Zhang, B. Zhang, J. Yao and S. Dai, *J. Phys. Chem. C.,* 2014, **118**, 8756.

37 Q. Wang, J. E. Moser and M. Grätzel, *J. Phys. Chem. B.*, 2005, **109**, 14945.

38 G. Wu, F. Kong, Y. Zhang, X. Zhang, J. Li, W. Chen, W. Liu, Y. Ding, C. Zhang, B. Zhang, J. Yao, S. Dai, *J. Phys. Chem. C.*, 2014, **118**, 8756.

39 W. Li, Y. Wu, Q. Zhang, H. Tian, W. Zhu, *ACS Appl. Mater. Interfaces.*, 2012, **4**, 1822.

40 Z-S. Wang, N. Koumura, Y. Cui, M. Takahashi, H. Sekiguchi, A. Mori, Toshitaka Kubo, A. Furube and K. Hara, *Chem. Mater.,* 2008, **20**, 3993.